Arrays of Nanoscale Lenses for Subwavelength Optical Lithography

ARTICLE *in* NANO LETTERS · SEPTEMBER 2010

Impact Factor: 13.59 · DOI: 10.1021/nl101942s · Source: PubMed

NANO LETTERS

pubs.acs.org/NanoLett

Arrays of Nanoscale Lenses for Subwavelength Optical Lithography

Jae-Won Jang,[†,ǂ,⊥,∥] Zijian Zheng,[†,ǂ,¶,∥] One-Sun Lee,[†,ǂ,∥] Wooyoung Shim,[ǂ,§] Gengfeng Zheng,[†,ǂ] George C. Schatz,[*,†,ǂ] and Chad A. Mirkin[*,†,ǂ,§]

[†]Department of Chemistry, [ǂ]International Institute for Nanotechnology, and [§]Department of Materials Science and Engineering, Northwestern University, 2145 Sheridan Road, Evanston, Illinois 60208-3113, United States

ABSTRACT Poly(ethylene glycol) (PEG) polymer lens arrays are made by using dip-pen nanolithography to deposit nanoscale PEG features on hydrophobically modified quartz glass. The dimensions of the PEG lenses are controlled by tuning dwell time and polymer molecular weight. The PEG polymer lenses on the quartz substrate act as a phase-shift photomask for fabricating subwavelength scale features, ~100 nm in width. Depending upon UV irradiation time during the photolithography, the photoresist nanostructures can be transitioned from well-shaped (short time) to ring-shaped (long time) features. The technique can be used to pattern large areas through the use of cantilever arrays.

KEYWORDS Dip-pen, lithography, poly(ethylene glycol), photomask, photoresist, phase-shift, nano, lens, finite element method, simulation

Patterning subwavelength features by photolithography in the far field is challenging because of the diffraction limit of light.[1,2] To overcome the diffraction limit, many patterning approaches have been developed, including near-field,[3] phase-shift,[4−7] and extreme ultraviolet photolithographic methods.[8] In particular, phase-shift photolithography, which employs polydimethylsiloxane (PDMS) as a photomask, is widely used because PDMS masks with nanoscale features can be made readily at relatively low-cost.[5−7] In addition to the phase-shift mask based photolithography approach, resolution in photolithography can be improved further by using mask materials, which act as nanoscale optical lenses. For example, Lee et al. reported recently how optical lenses of self-assembled calixarenes can be used in lithography to obtain subwavelength features.[9] The making and positioning of nanoscale lenses, with precise control over size distribution and substrate location, remain major challenges.

If there was a facile method for making nanoscale lenses and controlling their position on a substrate, one could create a powerful new way of using phase-shift photolithography to make nanoscale features with even better control over the position of the resulting features with respect to one another. Such capabilities could allow for rapid advances in the fabrication of electronics,[10] photonic structures,[11] and light harvesting materials.[12] Herein, we report a simple method for making nanoscale lenses from polyethylene glycol (PEG) with high substrate and pattern registration and excellent shape control using dip-pen nanolithography (DPN). Moreover, we show how the DPN-generated PEG nanolenses can be used as phase shift photomasks for patterning substrates with features having subwavelength dimensions.

DPN is a scanning-probe based lithography technique that allows one to pattern soft[13−26] and hard materials[27−29] with sub-50 nm to many micrometer resolution on a wide variety of substrates in a direct-write manner.[30−34] In a DPN experiment, an inked tip is used to transfer materials through a meniscus that naturally forms between the tip and substrate.[26,34,35] The chemisorption and in some cases strong physisorption of the ink on the underlying substrate facilitates ink transport and results in stable nanostructures.

Recently, we discovered that nanoscale features of PEG could be deposited by DPN in the form of plano-convex lenses on hydrophobic substrates such as hexamethyldisilazane (HMDS).[36,37] Since PEG is nearly transparent with a refractive index of ~1.43, we hypothesized that DPN with cantilever arrays could be used to generate nanoscale PEG lenses over large substrate areas,[30−32] and that such lenses could be used collectively as a phase-shift photomask. In principle, this approach would allow one to arbitrarily make any pattern with sub-100 nm resolution and near-perfect registration.

We evaluated the potential for using DPN to generate PEG masks comprising nanoscale features via a four-step procedure, Figure 1. First, HMDS is spin-coated onto a quartz substrate to generate a hydrophobic surface.[36] DPN is then used with a PEG-coated cantilever to precisely generate PEG lenses of a specific diameter and in a fixed pattern for

*To whom correspondence should be addressed. (C.A.M.) E-mail: chadnano@northwestern.edu. Phone: (847) 467-7302. (G.C.S.) E-mail: schatz@chem.northwestern.edu. Phone: (847) 491-5657.

∥ Equal contributions.

⊥ Current address: NanoInk, Inc., 8025 Lamon Avenue, Skokie, IL 60077.

¶ Current address: Institute of Textiles and Clothing, the Hong Kong Polytechnic University, Hung Hom, Kowloon, Hong Kong SAR.

Received for review: 06/1/2010
Published on Web: 09/29/2010

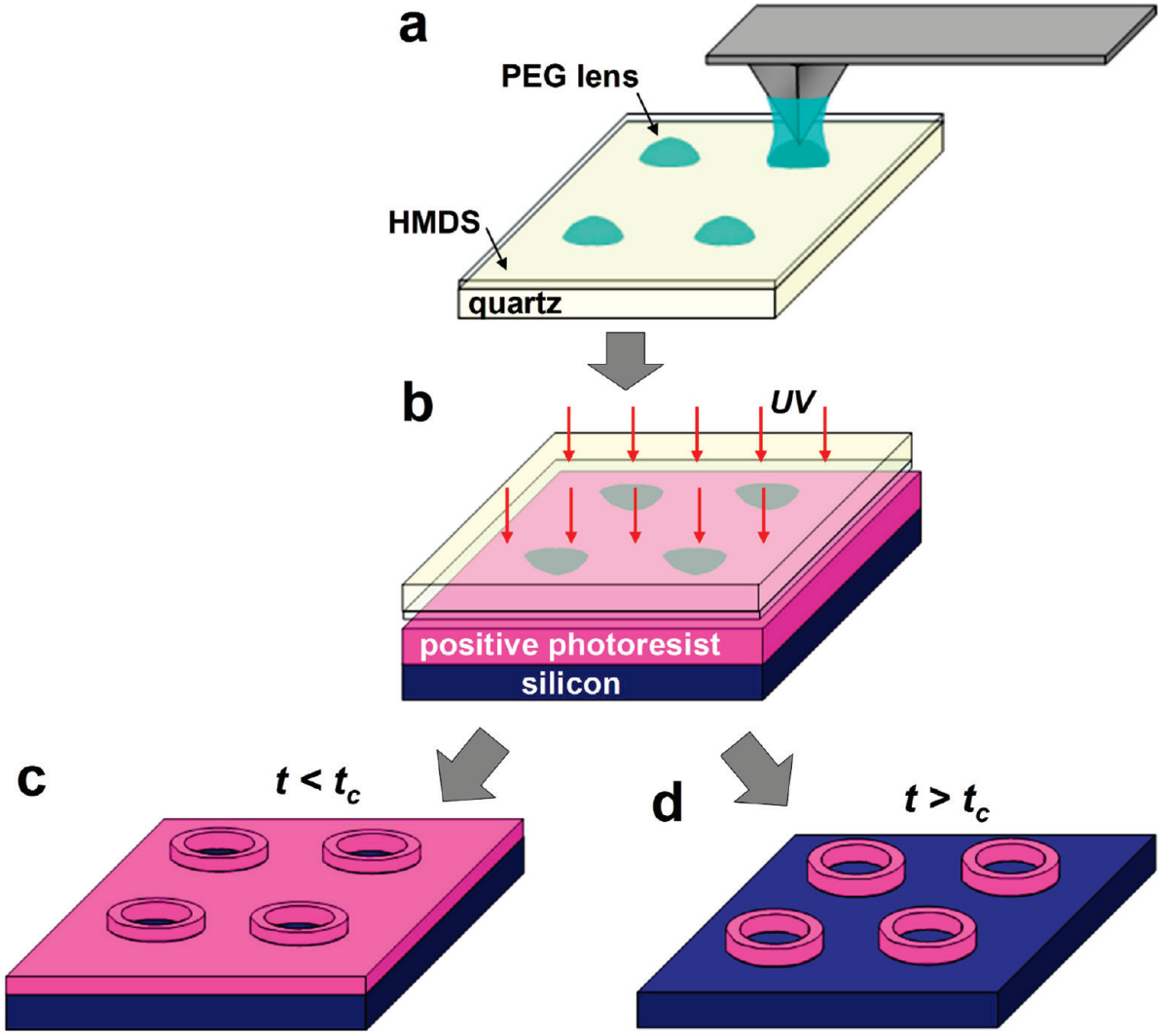

FIGURE 1. Schematic diagram showing the DPN patterning procedure used to make the PEG lens phase shift photomask. (a) Nanoscale PEG lenses are patterned on a HMDS-coated quartz glass substrate by DPN. (b) The PEG lenses focus UV light during the photolithography experiment. Since the UV intensity directly beneath the PEG lens is higher than the area around the edges, the type of resulting positive type photoresist features ((c) wells or (d) rings) are dependent upon UV exposure time.

subsequent use as a mask (Figure 1a). The size of each feature is controlled by contact time and the diffusion of PEG, and the details of this transport process have been described elsewhere.[36,37] The mask is then placed over an oxidized silicon wafer precoated with positive photoresist (S1805 with thickness of ~500 nm) and subsequently irradiated with 365 nm light. Each PEG lens focuses the irradiated UV light onto the positive photoresist, and the intensity of the UV light beneath the PEG lens is greater than the areas not covered by these nanoscale lenses (Figure 1b). There is also a drop in intensity of the light at the edges of the PEG lenses as observed with elastomeric phase-shift photolithography.[5−7] Since the intensity of light is higher beneath the PEG lens, the development of the photoresist beneath the PEG lens is substantially faster than areas not covered by PEG lenses. Therefore, this approach can be used to develop well- and ring-shaped photoresist features by controlling light exposure time. Specifically, if the exposure time is shorter than the critical resist development time (t_c), well-shaped photoresist features where the photoresist has not been totally removed are obtained. If the exposure time is longer than t_c, ring-shaped features are obtained (Figure 1c,d).

In a typical experiment, a 9 × 10 array of PEG lens features with 4 μm center-to-center distances was patterned by DPN on a HMDS-coated quartz glass using a 12-pen array (NanoInk Inc., Skokie, IL), where the sizes of the PEG lenses were deliberately adjusted by changing the dwell time of the tips (15, 10, 5, and 1 s) on the substrate at a fixed humidity of ~35% (Figure 2a). We studied the PEG material as a function of three different molecular weights: 2000, 35 000, and 100 000 Da. In general, the height of the nanoscale PEG lenses increases as the feature diameter increases (Figure 2b), and the aspect ratio of the resulting PEG lens at a fixed time increases with PEG molecular weight. This latter effect

DOI: 10.1021/nl101942s | *Nano Lett.* **2010,** *10,* 4399–4404

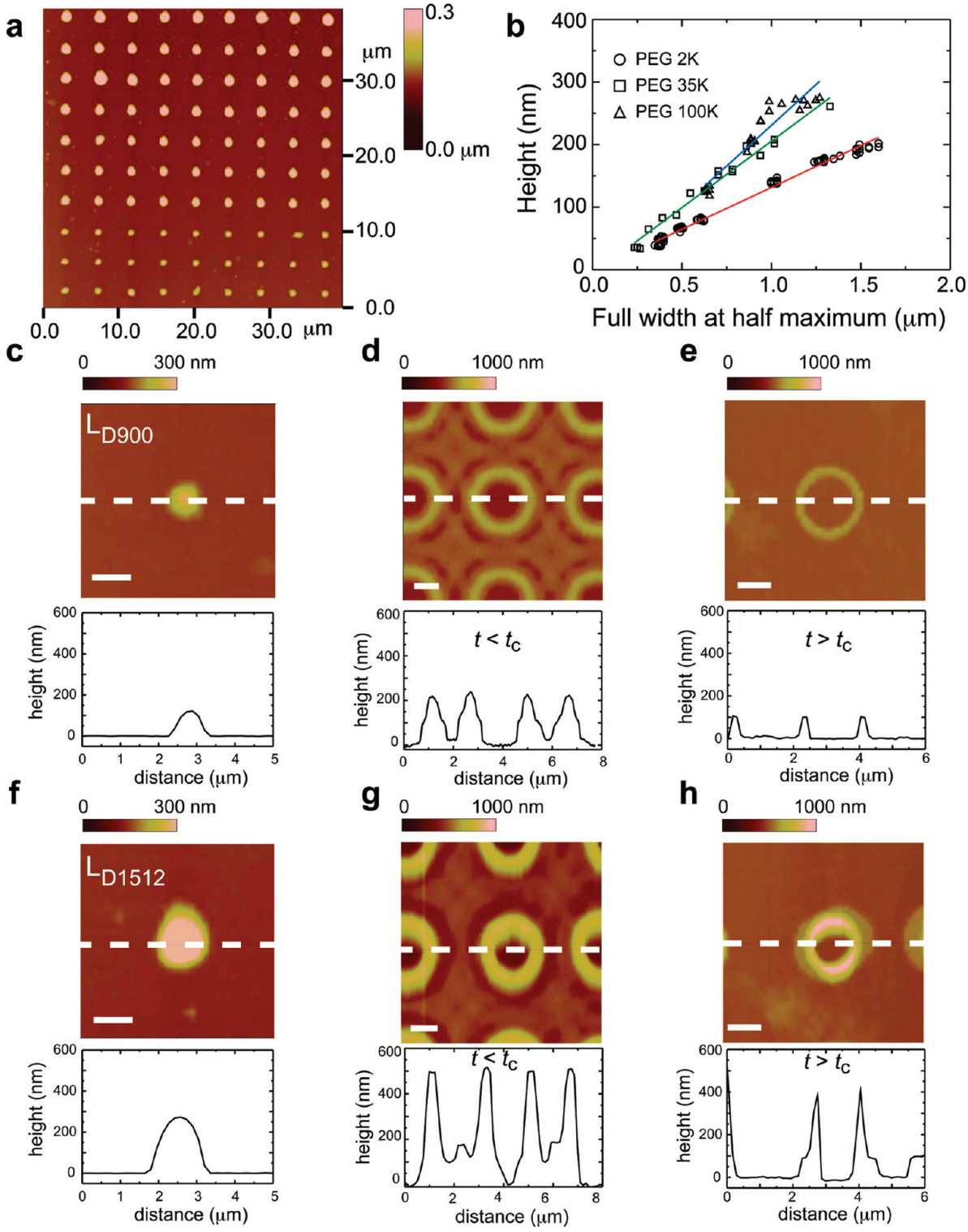

FIGURE 2. (a) Tapping mode AFM topographic image of the PEG nanoscale lenses generated by DPN. Lens size is dependent upon tip−substrate dwell time: 15 s (top row), 10 s (2nd to 4th row), 5 s (5th to 7th row), and 1 s (8th to 10th row). The PEG MW was 100 000 Da. (b) The relationship between the height and the full width at half-maximum (FWHM) of PEG lenses made from different polymer MWs on HMDS-coated quartz. (c) Tapping mode AFM topographic image and cross sectional line profiles of a PEG lens (MW = 100 000) with an average diameter of 900 nm (note only one lens is shown). The dwell time of the tip was 1 s. (d) The cross sectional profile of a positive photoresist feature generated from the PEG lenses in panel c with a UV exposure time of 3 s. (e) The positive photoresist feature generated when UV exposure time was 5 s. (f) Tapping mode AFM topographic image and cross sectional line profile of a PEG lens with a diameter of 1512 nm (dwell time was 15 s). (g) The cross-sectional line profile of a positive photoresist feature generated by a PEG lens like the one in f with a UV exposure time of 3 s. (h) A similar feature, but after a UV exposure time of 5 s. The path for the AFM cross section line profiles are denoted by the white dashed lines. The length of the scale bar in each figure is 1 μm. All AFM images were done using ultrasharp tips (2 nm radius).

DOI: 10.1021/nl101942s | *Nano Lett.* **2010,** *10,* 4399–4404

is a consequence of the increased viscosity of the higher molecular weight PEG.[38]

The performance of the phase-shift photomask made by a DPN-patterned PEG lens array in Figure 2a was evaluated by conventional photolithography ($\lambda = 365$ nm) on a silicon wafer prespincoated with a positive type photoresist (S1805, MicroChem. Inc.). Two sizes of PEG lenses, patterned at 1 and 15 s DPN dwell times and having diameters of 900 and 1512 nm (denoted as L_{D900} and L_{D1512} in Figure 2c,f), respectively, were selected as examples for investigating the relationship between the PEG lens dimensions and the photoresist features. For the photoresist pattern with 3 s exposure, well-shaped photoresist features were fabricated (Figure 2d,g). On the other hand, ring-shaped features were obtained with 5 s of UV exposure (Figure 2e,h). As hypothesized, these two different types of photoresist features can be made simply by changing exposure time, where t_c is ~4 s. Moreover, we found that the dimensions of the developed photoresist feature are significantly affected by the size of the PEG lenses. In general, the diameters of the photoresist features decrease as the diameters of the PEG lens increase, whereas the heights of the photoresist features increase as the heights of the PEG lenses increase. For more detailed analysis, see Figure S3 in the Supporting Information.

To obtain a deeper understanding of the system, the UV intensity profile inside the photoresist was calculated using the finite element method (FEM) with a two-dimensional model.[39−41] Two samples of PEG lenses (L_{D900} and L_{D1512} in Figure 2c,f) were selected for the simulation. The cross sectional profile from the AFM image of each sample was fitted to a spherical shape to obtain a lens radius (Figure S4 in Supporting Information), yielding 894 nm for L_{D900} and 1170 nm for L_{D1512}. It was assumed that the bottom of the PEG lens is in contact with the photoresist surface in the calculations. Intensity profiles were determined at this photoresist surface and down to a 500 nm depth below the surface at intervals of 100 nm. (The typical thickness of the S1805 photoresist is ~500 nm). The resulting UV intensity profiles are shown in Figure 3a,b with details of the model shown in the inset of Figure 3a. The profiles show that the light intensity beneath the PEG lens is higher than in areas not covered by the PEG lens throughout the photoresist layer. A minimum light intensity is found near the edges of the PEG lens, which is consistent with the experiments in Figure 2. This minimum intensity is also consistent with previous reports that show a minimum light intensity profile at the edges of a rectangular-shaped elastomeric phase shift photomask.[6,7]

The FEM simulations also predict the formation of well- or ring-shaped photoresist features, depending upon irradiation time. To model our experiments, we used FEM to calculate the focal length of the PEG lens. The calculations show that the focal length is only 40−80% of the value obtained using the geometric optics equation (See Figure S5 in the Supporting Information for more details), which is

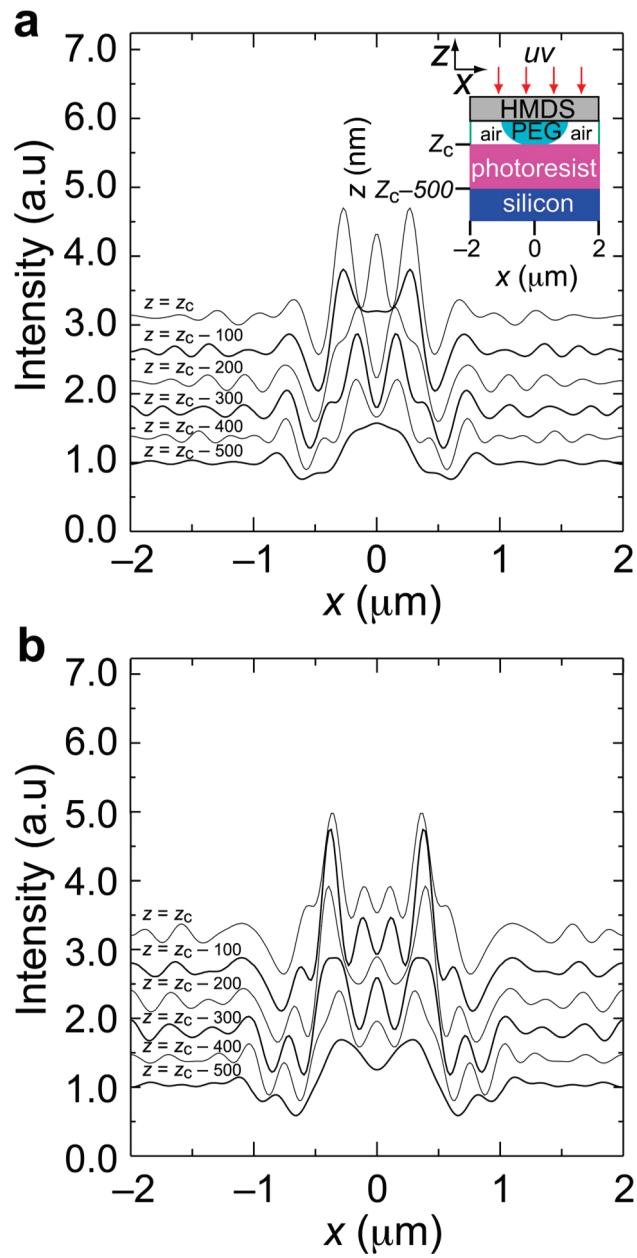

FIGURE 3. Intensity of light in the photoresist is calculated for (a) L_{D900} and (b) L_{D1512} using FEM. The photomask in contact with the layer of photoresist is used in the simulation. The model used is shown in the inset of panel a. The profile of light intensity is obtained from the surface of photoresist that contacts with the PEG lens (Z_c) to the bottom of the photoresist (Z_c − 500 nm) at intervals of 100 nm.

similar to previously reported results for nanoscale lenses.[9] The attenuation of light, however, in the photoresist reduces the focusing properties of the PEG lens when used for the calculations in Figure 3 such that the intensity of the pattern is largely suppressed at 500 nm below the surface.

For features with subwavelength dimensions, an array of ring-shaped photoresist structures with 100 nm thick walls was fabricated (Figure 4a,b). The array was made by using a phase-shift photomask comprised of ~1.3 μm diameter

DOI: 10.1021/nl101942s | *Nano Lett.* **2010,** *10,* 4399–4404

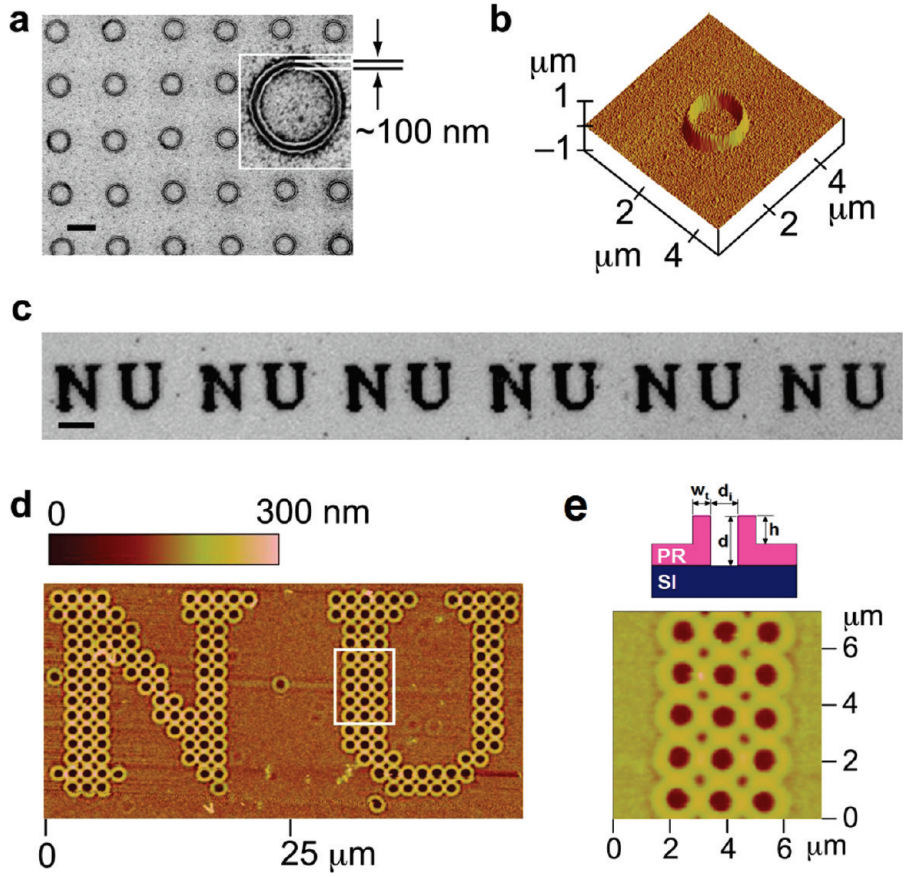

FIGURE 4. (a) SEM image of ring-shaped photoresist features fabricated from a phase-shift photomask made of DPN-patterned PEG lenses with a UV exposure time of 6.5 s. The average wall thickness of each ring is ~100 nm. The scale bar is 2 μm. (b) Tapping mode AFM topography images of panel a. (c) Optical microscope image of a photoresist pattern in the form of an NU logo fabricated with a PEG lens array phase shift photomask: a one-dimensional tip array (6 tips) was used to generate the phase shift photomask. The scale bar is 20 μm. (d) AFM topography images of the NU logo photoresist pattern, consisting of 182 photoresist well features with a 1.5 μm average center-to-center distance. The MW of the PEG was 35 000 Da. Features outside the NU letters are errors that originate from small dust particles on the photomask. (e) A higher magnification image of the region denoted with the white box in panel d. All AFM images were done using ultrasharp tips (2 nm radius).

DPN-deposited PEG lenses (MW = 35 000 Da), and the photomask was irradiated with 365 nm light. Photoresist patterns consisting of well-shaped structures were also fabricated by conventional photolithography by using an array of DPN generated PEG lenses (Figure 4c−e). The array in this case was fabricated using a parallel DPN printing method that employed a one-dimensional 6-pen array. PEG lenses (1,092 units) were generated on the HMDS-coated quartz glass substrate within 10 min using this method, and AFM measurements photoresist structures (nanowell arrays) post-photolithography show that they are uniform and highly ordered. The average internal diameter (d_i) of each nanowell is 734 ± 8 nm, the average wall thickness (w_t) is 398 ± 21 nm, the average height (h) is 44 ± 2 nm, and the average depth (d) is 104 ± 3 nm (Figure 4e).

In conclusion, DPN allows one to pattern arrays of PEG nanoscale lens with precise positioning and feature dimension control. These novel PEG nanolenses can be used with conventional photolithography to generate subwavelength features with near perfect registration. This technique may be useful for the fabrication of high quality nano- and microstructures not easily obtainable by conventional methods.[30−32] Moving forward, an investigation of the relationship between lens feature shape and resulting feature control will be needed to fully exploit the new capabilities afforded by this technique.

Acknowledgment. This research was supported by the National Science Foundation through Grant CHE-0843832 and the Northwestern NSEC Center (NSF Grant EEC-0647560). C.A.M. also acknowledges the AFOSR and DARPA for financial support. We thank professors J. Rogers and S. Jeon for helpful discussion and Professor S. Hong for sharing his software code for the FEM simulations.

Supporting Information Available. Experimental Section, additional figures, and additional references. This material is available free of charge via the Internet at http://pubs.acs.org.

DOI: 10.1021/nl101942s | *Nano Lett.* **2010,** *10,* 4399–4404

REFERENCES AND NOTES

(1) Abbé, E. *Arch. Mikrosk. Anat. Entwichlungsmech.* **1873**, *9*, 413–418.
(2) Wang, W. C. M.; Stoltenberg, R. M.; Liu, S. H.; Bao, Z. N. *ACS Nano* **2008**, *2*, 2135–2142.
(3) Alkaisi, M. M.; Blaikie, R. J.; McNab, S. J.; Cheung, R.; Cumming, D. R. S. *Appl. Phys. Lett.* **1999**, *75*, 3560–3562.
(4) Levenson, M. D.; Viswanathan, N. S.; Simpson, R. A. *IEEE Trans. Electron Devices* **1982**, *29*, 1828–1836.
(5) Odom, T. W.; Thalladi, V. R.; Love, J. C.; Whitesides, G. M. *J. Am. Chem. Soc.* **2002**, *124*, 12112–12113.
(6) Rogers, J. A.; Paul, K. E.; Jackman, R. J.; Whitesides, G. M. *Appl. Phys. Lett.* **1997**, *70*, 2658–2660.
(7) Rogers, J. A.; Paul, K. E.; Jackman, R. J.; Whitesides, G. M. *J. Vac. Sci. Technol.* **1998**, *16*, 59–68.
(8) Cerrina, F.; Guckel, H.; Wiley, J. D.; Taylor, J. W. *J. Vac. Sci. Technol., B* **1985**, *3*, 227–231.
(9) Lee, J. Y.; Hong, B. H.; Kim, W. Y.; Min, S. K.; Kim, Y.; Jouravlev, M. V.; Bose, R.; Kim, K. S.; Hwang, I.-C.; Kaufman, L. J.; Wong, C. W.; Kim, P.; Kim, K. S. *Nature* **2009**, *460*, 498–501.
(10) Fan, Z. Y.; Ho, J. C.; Jacobson, Z. A.; Razavi, H.; Javey, A. *Proc. Natl. Acad. Sci. U.S.A.* **2008**, *105*, 11066–11070.
(11) Shir, D. J.; Jeon, S.; Liao, H.; Highland, M.; Cahill, D. G.; Su, M. F.; El-Kady, I. F.; Christodoulou, C. G.; Bogart, G. R.; Hamza, A. V.; Rogers, J. A. *J. Phys. Chem. B* **2007**, *111*, 12945–12958.
(12) Huang, F. M.; Zheludev, N.; Chen, Y. F.; de Abajo, F. J. G. *Appl. Phys. Lett.* **2007**, *90*, No. 091119.
(13) Zhang, H.; Li, Z.; Mirkin, C. A. *Adv. Mater.* **2002**, *14*, 1472–1474.
(14) Wang, Y. H.; Maspoch, D.; Zou, S. L.; Schatz, G. C.; Smalley, R. E.; Mirkin, C. A. *Proc. Natl. Acad. Sci. U.S.A.* **2006**, *103*, 2026–2031.
(15) Sheehan, P. E.; Whitman, L. J.; King, W. P.; Nelson, B. A. *Appl. Phys. Lett.* **2004**, *85*, 1589–1591.
(16) Rozhok, S.; Piner, R.; Mirkin, C. A. *J. Phys. Chem. B* **2003**, *107*, 751–757.
(17) Liu, X. G.; Guo, S. W.; Mirkin, C. A. *Angew. Chem., Int. Ed.* **2003**, *42*, 4785–4789.
(18) Lim, J. H.; Mirkin, C. A. *Adv. Mater.* **2002**, *14*, 1474–1477.
(19) Lim, J. H.; Ginger, D. S.; Lee, K. B.; Heo, J.; Nam, J. M.; Mirkin, C. A. *Angew. Chem., Int. Ed.* **2003**, *42*, 2309–2312.
(20) Lee, K. B.; Park, S. J.; Mirkin, C. A.; Smith, J. C.; Mrksich, M. *Science* **2002**, *295*, 1702–1705.
(21) Jung, H.; Kulkarni, R.; Collier, C. P. *J. Am. Chem. Soc.* **2003**, *125*, 12096–12097.
(22) Jang, J. W.; Sanedrin, R. G.; Maspoch, D.; Hwang, S.; Fujigaya, T.; Jeon, Y. M.; Vega, R. A.; Chen, X. D.; Mirkin, C. A. *Nano Lett.* **2008**, *8*, 1451–1455.
(23) Jang, J. W.; Maspoch, D.; Fujigaya, T.; Mirkin, C. A. *Small* **2007**, *3*, 600–605.
(24) Demers, L. M.; Park, S. J.; Taton, T. A.; Li, Z.; Mirkin, C. A. *Angew. Chem., Int. Ed.* **2001**, *40*, 3071–3073.
(25) Demers, L. M.; Ginger, D. S.; Park, S. J.; Li, Z.; Chung, S. W.; Mirkin, C. A. *Science* **2002**, *296*, 1836–1838.
(26) Piner, R. D.; Zhu, J.; Xu, F.; Hong, S. H.; Mirkin, C. A. *Science* **1999**, *283*, 661–663.
(27) Wang, H. T.; Nafday, O. A.; Haaheim, J. R.; Tevaarwerk, E.; Amro, N. A.; Sanedrin, R. G.; Chang, C. Y.; Ren, F.; Pearton, S. J. *Appl. Phys. Lett.* **2008**, *93*, 143105.
(28) Liu, S. T.; Maoz, R.; Sagiv, J. *Nano Lett.* **2004**, *4*, 845–851.
(29) Li, B.; Goh, C. F.; Zhou, X. Z.; Lu, G.; Tantang, H.; Chen, Y. H.; Xue, C.; Boey, F. Y. C.; Zhang, H. *Adv. Mater.* **2008**, *20*, 4873–4878.
(30) Salaita, K.; Wang, Y. H.; Fragala, J.; Vega, R. A.; Liu, C.; Mirkin, C. A. *Angew. Chem., Int. Ed.* **2006**, *45*, 7220–7223.
(31) Salaita, K.; Lee, S. W.; Wang, X. F.; Huang, L.; Dellinger, T. M.; Liu, C.; Mirkin, C. A. *Small* **2005**, *1*, 940–945.
(32) Huo, F. W.; Zheng, Z. J.; Zheng, G. F.; Giam, L. R.; Zhang, H.; Mirkin, C. A. *Science* **2008**, *321*, 1658–1660.
(33) Salaita, K.; Wang, Y. H.; Mirkin, C. A. *Nat. Nanotechnol.* **2007**, *2*, 145–155.
(34) Mirkin, C. A. *ACS Nano* **2007**, *1*, 79–83.
(35) Ginger, D. S.; Zhang, H.; Mirkin, C. A. *Angew. Chem., Int. Ed.* **2004**, *43*, 30–45.
(36) Jang, J.-W.; Sanedrin, R. G.; Senesi, A. J.; Zheng, Z.; Chen, X.; Hwang, S.; Huang, L.; Mirkin, C. A. *Small* **2009**, *5*, 1850–1853.
(37) Zheng, Z.; Jang, J. W.; Zheng, G.; Mirkin, C. A. *Angew. Chem., Int. Ed.* **2008**, *47*, 9951–9954.
(38) Brandrup, J.; Immergut, E. H. *Polymer Handbook*; John Wiley and Sons: New York, 1989.
(39) Dahlquist, G.; Bjorck, A. *Numerical methods*; Prentice-Hall, Inc.: Englewood Cliffs, NJ, 1974.
(40) Monk, P. *Finite Element Methods for Maxwell's Equations*; Oxford University Press: New York, 2003.
(41) Yee, K. S. *IEEE Trans. Antennas Propag.* **1966**, *AP14*, 302–307.

DOI: 10.1021/nl101942s | *Nano Lett.* **2010,** *10,* 4399–-4404